

Received September 22, 2019, accepted September 28, 2019, date of publication October 1, 2019,  
date of current version November 14, 2019.

Digital Object Identifier 10.1109/ACCESS.2019.2944894

# Path Tracking Control for Autonomous Vehicles Based on an Improved MPC

HENGYANG WANG<sup>ID</sup><sup>1</sup>, BIAO LIU<sup>ID</sup><sup>1</sup>, XIANYAO PING<sup>2</sup>, AND QUAN AN<sup>2</sup>

<sup>1</sup>School of Electrical Engineering, Beijing Jiaotong University, Beijing 100044, China

<sup>2</sup>School of Vehicle and Mobility, Tsinghua University, Beijing 100084, China

Corresponding author: Biao Liu (liubiao@bjtu.edu.cn)

This work was supported in part by the Fundamental Research Funds for the Central Universities under Grant 2019YJS178.

**ABSTRACT** In this paper, an improved Model Predictive Control (MPC) controller based on fuzzy adaptive weight control is proposed to solve the problem of autonomous vehicle in the process of path tracking. The controller not only ensures the tracking accuracy, but also considers the vehicle dynamic stability in the process of tracking, i.e., the vehicle dynamics model is used as the controller model. Moreover, the problem of driving comfort caused by the application of classical MPC controller when the vehicle is deviated from the target path is solved. This controller is mainly realized by adaptively improving the weight of the cost function in the classical MPC through the fuzzy adaptive control algorithm. A comparative study which compares the proposed controller with the pure-pursuit controller and the classical MPC controller is made: through the CarSim-Matlab/Simulink co-simulations, the results show that this controller presents better tracking performance than the latter ones considering both tracking accuracy and steering smoothness.

**INDEX TERMS** Autonomous vehicles, path tracking, improved MPC controller, weight adaptive control.

## I. INTRODUCTION

Autonomous vehicle, a product of the integration of advanced sensing technology, artificial intelligence technology and the latest control technology in the automotive industry, plays a key role in enhancing ride comfort [1], optimizing resource consumption and pollution emission [2], and, most importantly, increasing driving safety [3], [4], which has attracted enough attention from governments, universities and enterprises [5]. As one of the most essential operating conditions of driverless cars, path tracking aims to assure that the vehicle can be guided to follow a predetermined trajectory that can be generated offline through a navigation system or online through a path-planning method by manipulating steering wheel at a certain speed [6], [7]. Tracking accuracy and steering smoothness are two key criteria in designing tracking algorithms which also take into consideration the multivariable and nonlinear characteristics of this problem [8], [9].

At present, the main control strategies include proportion integration differentiation (PID) control, fuzzy logic control and MPC method. Chaib *et al.* [10] analyzed and compared the following performance between PID control and fuzzy

The associate editor coordinating the review of this manuscript and approving it for publication was Jianyong Yao<sup>ID</sup>.

logic control under different adhesion coefficients by simulation. In [11], a robust PID controller is constructed to effectively control a mobile robot that travels along the given path by using a simplified robot model composed of an integrator and a delay. Considering that multiple control tasks (e.g. tracking accuracy, ride comfort and driving stability), PID controller is not the optimal control method for the path tracking of autonomous car owing to no capacity for dealing with several control objectives. Naranjo *et al.* [12] proposed a fuzzy controller mimicking human behavior and reactions to accomplish an overtaking condition which consists of changes between two lanes—one from the right to the left lane of the road, and the other is to return to the right lane after overtaking. A fuzzy controller is presented to improve vehicle yaw stability by actively controlling the front steering angle and the distribution of braking forces [13].

The path tracking problem, as a multi-constrained optimization problem, needs to take into account not only the location error constraint in the tracking process, but also the comfort constraint and the mechanical and electrical parts. Model predictive controller (MPC) algorithm establishing multivariable cost function under future reference state conditions and minimizing the function with respect to multiple constraints has drawn a lot of interest in the domain of unmanned vehicle control. A MPC controller whose weight

matrix is controlled by a stability-coefficient adaptively is proposed to control the accuracy of car-following and lateral dynamic stability of vehicles under ACC conditions in curved lanes [14]. Raffo *et al.* [6] used MPC strategy considering both the kinematic and dynamic models in a cascade structure to keep an autonomous vehicle tracking along the predetermined trajectory, which focused on tracking performance and hardware consumption. A vehicle equipped with an embedded computing system verified the effectiveness of this method. In [15], J. Ji *et al.* proposed a collision avoidance architecture on the road containing path planning and path tracking. On the one hand, a 3D virtual dangerous potential field method with repulsive potential resulting from all obstacles and attractive potential from safe zones was designed to generate a reference trajectory avoiding collision with the front car for the path tracking layer. Next, a MMPC (Multi-constrained Model Predictive Control) controller regulated the autonomous vehicle to track the target path from the path planning layer to complete collision avoidance process. Some improvement methods for MPC have been studied. for example, the weight matrices in the MPC cost function can be adjusted according to the control mode, which can not only ensure the ride comfort of vehicles in normal driving mode, but also effectively avoid collision in emergency situations [16]. a robust tube-based model predictive control (RMPC) approach is proposed to improve directional stability performance of the vehicle after a tire blowout on curved expressway in [17].

Although the MPC strategy can ensure the high tracking accuracy during tracking maneuver, the driving comfort problem caused by fixed weight in cost function in classical MPC when the vehicle is far away from the desired path has seldom been studied. To guarantee high tracking accuracy and improve ride comfort, we raise an improved MPC strategy to deal with the path tracking problem, which adaptively controls the weight of the cost function by using fuzzy adaptive control algorithm. The simulation results show that the algorithm can match the target criteria better.

The remainder of this paper is organized as follows: Section II describes the vehicle model used in proposed controller, i.e., Vehicle Dynamics Model. In section III, a predictive optimization problem is established considering tracking accuracy, ride comfort and vehicle stability, which is based on MPC structure. Section IV highlights how to apply fuzzy adaptive control algorithm to control the weight of the cost function in classical MPC. Section V depicts the obtained experimental results compared with pure-pursuit algorithm. Finally, conclusions are presented in Section VI.

## II. MATHEMATICAL MODEL

Path tracking problem is very dependent on vehicle model since it is an important requirement for MPC method. In this section, we will introduce the vehicle model and tire model used in control strategy and the corresponding derivation process. The bicycle model of an Ackerman steered vehicle [18] is a simple and effective vehicle model which has been

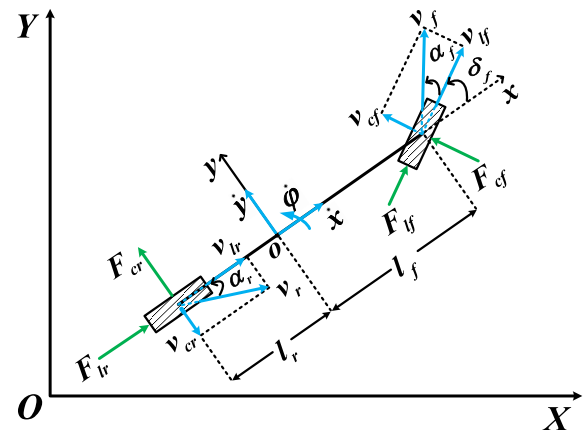


**FIGURE 1.** Vehicle dynamics model. XOY represents inertial coordinate system and xoy is the local body-fixed coordinate system.

**TABLE 1.** Symbols and definitions in bicycle model.

Symbol	Definition
$m$	Vehicle weight
$\delta_f$	Front wheel steering angle
$\alpha_f/\alpha_r$	Front / rear wheel sideslip angle
$l_f/l_r$	Distance from center of mass to front / rear axle
$\dot{x}$	Vehicle longitudinal speed (in xoy)
$\dot{y}$	Vehicle lateral speed (in xoy)
$v_{lf}/v_{lr}$	Longitudinal speed of front / rear wheel
$v_{cf}/v_{cr}$	Lateral speed of front / rear wheel
$\dot{\phi}$	Yaw rate
$F_{lf}/F_{lr}$	Longitudinal force on front / rear tires
$F_{cf}/F_{cr}$	Lateral force on front / rear tires

widely used in vehicle stability control as shown in Fig. 1. To apply this model, some simplifications should be considered: 1) The wheels of the same axle are lumped in a single wheel located in the center of the front or rear axle. 2) The weight of the body is evenly distributed on each wheel. 3) Suspension movements, slip phenomena, and aerodynamic influences are neglected. The definitions in vehicle model are listed in Table 1.

Applying Newton's Second Law to longitudinal, lateral, and yaw degrees of freedom [19], vehicle dynamics model can be constructed:

$$\begin{cases} m\ddot{x} = m\dot{y}\dot{\phi} + 2(F_{lf} \cos \delta_f - F_{cf} \sin \delta_f) + 2F_{lr} \\ m\ddot{y} = -m\dot{x}\dot{\phi} + 2(F_{lf} \sin \delta_f + F_{cf} \cos \delta_f) + 2F_{cr} \\ I_z\ddot{\phi} = 2l_f(F_{lf} \sin \delta_f + F_{cf} \cos \delta_f) - 2l_rF_{cr} \end{cases} \quad (1)$$

where  $I_z$  denotes yaw inertia. In addition to the effects of aerodynamic forces and gravity, the other forces acting on the car come from the tires. Thus, it is very essential to choose a tire model that is close to the reality. In order to solve the lateral and longitudinal forces on tires, a Pacejka tire model is applied in this paper, which is a semi-empirical nonlinear model [16], [20]. When the cornering angle and slip ratio of tire are small, the linearized and simplified formulas of longitudinal force and lateral force in the tire model are

given by:

$$\begin{cases} F_{lf} = C_{lf} s_f \\ F_{cf} = C_{cf} \alpha_f \\ F_{lr} = C_{lr} s_r \\ F_{cr} = C_{cr} \alpha_r \end{cases} \quad (2)$$

where  $C_{lf}/C_{lr}$  is longitudinal stiffness of front / rear tire,  $C_{cf}/C_{cr}$  is lateral stiffness,  $s_f/s_r$  indicates tire slip rate,  $\alpha_f/\alpha_r$  represents side slip angle of front and rear tire respectively. From the geometric relations in Fig. 1, we derive:

$$\begin{cases} \alpha_f = \tan^{-1} \frac{v_{cf}}{v_{lf}} \\ \alpha_r = \tan^{-1} \frac{v_{cr}}{v_{lr}} \end{cases} \quad (3)$$

where

$$\begin{cases} v_{cf} = (\dot{y} + l_f \dot{\phi}) \cos \delta_f - \dot{x} \sin \delta_f \\ v_{lf} = (\dot{y} + l_f \dot{\phi}) \sin \delta_f + \dot{x} \cos \delta_f \\ v_{cr} = l_r \dot{\phi} - \dot{y} \\ v_{lr} = \dot{x} \end{cases} \quad (4)$$

When the front wheel angle is small, from Eq. (1)-(4), the nonlinear dynamic model of vehicle is established:

$$m\ddot{x} = m\dot{y}\dot{\phi} + 2 \left[ C_{lf} s_f + C_{cf} \left( \delta_f - \frac{\dot{y} + l_f \dot{\phi}}{\dot{x}} \right) \delta_f + C_{lr} s_r \right] \quad (5)$$

$$\begin{aligned} m\ddot{y} = & -m\dot{x}\dot{\phi} \\ & + 2 \left[ C_{lf} s_f \delta_f + C_{cf} \left( \frac{\dot{y} + l_f \dot{\phi}}{\dot{x}} - \delta_f \right) + C_{cr} \frac{l_r \dot{\phi} - \dot{y}}{\dot{x}} \right] \end{aligned} \quad (6)$$

$$I_z \ddot{\phi} = 2l_f \left[ C_{lf} s_f \delta_f + C_{cf} \left( \frac{\dot{y} + l_f \dot{\phi}}{\dot{x}} - \delta_f \right) \right] - 2l_r C_{cr} \frac{l_r \dot{\phi} - \dot{y}}{\dot{x}} \quad (7)$$

Converting the vehicle motion in local body-fixed coordinate system to inertial system [20]:

$$\dot{X} = \dot{x} \cos \varphi - \dot{y} \sin \varphi \quad (8)$$

$$\dot{Y} = \dot{x} \sin \varphi + \dot{y} \cos \varphi \quad (9)$$

The mathematical model of an improved MPC controller applied to path tracking is shown in Eq. (5)-(9), which is a nonlinear continuous model.

### III. MODEL PREDICTIVE CONTROL

Linear model predictive control (LMPC) is used as a basic controller strategy to solve the problem of path tracking in this section, which has higher computational efficiency compared with NMPC (Non-linear MPC) [6]. The objective of MPC is to calculate a series of control sequence in the prediction horizon, in this way, the error between the output and the reference is reduced as many as possible, i.e., in the process of path tracking, it minimizes the gap between the reference path and the trajectory predicted by the vehicle dynamics model. This is achieved by solving a quadratic programming problem considering multiple constraints.

The solving process of Linear MPC algorithm can be generally divided into four parts. First of all, because the discrete state-space model is generally adopted for the controlled system in MPC [19], nonlinear continuous state model of vehicle in section II should be linearized and discretized. Next, the state variables and output variables need to be predicted at each time step, which will be compared with the corresponding reference variables. Then, the cost function is developed taking into account a set of constraints between the control actions and the outputs. A quadratic programming procedure will be resolved finally.

#### A. MODEL LINEARIZATION AND DISCRETIZATION

In order to guarantee the stability of the vehicle when tracing, the vehicle dynamics model in the previous section is utilized to design the upper MPC controller. The six-state space variable vector can be recorded as  $\chi = [\dot{x}, \dot{y}, \varphi, \dot{\varphi}, X, Y]^T$  and steering angle is used as the control variable,  $u = \delta_f$  [21]. The linearized state equations based on Eq. (5)-(9) are obtained as follows [22]:

$$\dot{\chi}_t = A_t \chi_t + B_t u_t \quad (10)$$

$$Y_t = C_t \chi_t \quad (11)$$

where

$$B_t = \begin{bmatrix} \frac{2C_{cf}(2\delta_f - \frac{\dot{y} + l_f \dot{\phi}}{\dot{x}})}{m} \\ \frac{2(C_{lf} s_f - C_{cf})}{m} \\ 0 \\ \frac{2l_f(C_{lf} s_f - C_{cf})}{I_z} \\ 0 \\ 0 \end{bmatrix} \quad (13)$$

$$A_t = \begin{bmatrix} \frac{2C_{cf}\delta_{f,t-1}(\dot{y} + l_f \dot{\phi})}{m(\dot{x}_t)^2} & \dot{\varphi}_t - \frac{2C_{cf}\delta_f}{m\dot{x}} & 0 & \dot{y} - \frac{2C_{cf}l_f\delta_f}{m\dot{x}} & 0 & 0 \\ -\dot{\varphi} - \frac{2C_{cf}(\dot{y} + l_f \dot{\phi}) + 2C_{cr}(l_r \dot{\phi} - \dot{y})}{m(\dot{x})^2} & \frac{2C_{cf} - 2C_{cr}}{m\dot{x}} & 0 & -\dot{x} + \frac{2(C_{cf}l_f + C_{cr}l_r)}{m\dot{x}} & 0 & 0 \\ 0 & 0 & 0 & 1 & 0 & 0 \\ \frac{2l_r C_{cr}(l_r \dot{\phi} - \dot{y}) - 2l_f C_{cf}(\dot{y} + l_f \dot{\phi})}{I_z(\dot{x})^2} & \frac{2l_f C_{cf} + 2l_r C_{cr}}{I_z \dot{x}} & 0 & \frac{2(C_{cf}l_f^2 - C_{cr}l_r^2)}{I_z \dot{x}} & 0 & 0 \\ \cos \varphi & -\sin \varphi & -\dot{x} \sin \varphi - \dot{y} \cos \varphi & 0 & 0 & 0 \\ \sin \varphi & \cos \varphi & \dot{x} \cos \varphi - \dot{y} \sin \varphi & 0 & 0 & 0 \end{bmatrix} \quad (12)$$

$$Y_t = \begin{bmatrix} \varphi \\ Y \end{bmatrix} C_t = \begin{bmatrix} 0 & 0 & 1 & 0 & 0 & 0 \\ 0 & 0 & 0 & 0 & 0 & 1 \end{bmatrix} \quad (14)$$

We discretize the model based on Eq. (10), (11) into a discrete, single-input, multi-output model using Euler method. The discrete state-space equation can be obtained:

$$\chi(k+1) = A_k \chi(k) + B_k u(k) \quad (15)$$

$$Y(k) = C_k \chi(k) \quad (16)$$

where  $A_k$ ,  $B_k$  and  $C_k$  represent state matrix, control matrix and output matrix respectively. The equation can be presented as follows:

$$\begin{cases} A_k = e^{A_t T_s} \\ B_k = \int_0^{T_s} e^{A\tau} d\tau \cdot B_t \\ C_k = C_t \end{cases} \quad (17)$$

### B. STATE AND OUTPUT PREDICTION

In the process of path tracking, we need to predict the future behavior of vehicle in the specified prediction horizon, and calculate the control input in the next moment by minimizing the error between predictive variables and the references under various constraints.

Owing to the mechanical constraints of automobiles, a new state-space expression is established based on Eq. (15), (16), in which the increment of control ( $\Delta u$ ) is selected as the input variable. Meanwhile, the state-space variable  $\chi(k)$  and the control variable  $u(k-1)$  are augmented as the new state variable  $\tilde{\chi}(k)$ . The new state-space expression is presented as follows:

$$\tilde{\chi}(k+1) = \tilde{A}_k \tilde{\chi}(k) + \tilde{B}_k \Delta u(k) \quad (18)$$

$$\tilde{Y}(k) = \tilde{C}_k \tilde{\chi}(k) \quad (19)$$

where

$$\begin{cases} \tilde{\chi}(k) = \begin{bmatrix} \chi(k) \\ u(k-1) \end{bmatrix}, & \Delta u(k) = u(k) - u(k-1) \\ \tilde{A}_k = \begin{bmatrix} A_k & B_k \\ 0_{1 \times 6} & I \end{bmatrix}, & \tilde{B}_k = \begin{bmatrix} B_k \\ I \end{bmatrix} \\ \tilde{C}_k = \begin{bmatrix} C_k & 0 \end{bmatrix}, & \tilde{Y}(k) = Y(k) \end{cases} \quad (20)$$

The prediction horizon and control horizon of the upper decision controller based on MPC are set to  $N_P$  and  $N_c$ ,

$$\begin{aligned} \tilde{\chi}(k+1|k) &= \tilde{A}_k \tilde{\chi}(k) + \tilde{B}_k \Delta u(k) \\ \tilde{\chi}(k+2|k) &= \tilde{A}_{k+1} \tilde{A}_k \tilde{\chi}(k) + \tilde{A}_k \tilde{B}_k \Delta u(k) + \tilde{B}_{k+1} \Delta u(k+1) \\ &\vdots \\ \tilde{\chi}(k+N_c|k) &= \alpha(k, N_c-1, 0) \tilde{\chi}(k) + \alpha(k, N_c-1, 1) \tilde{B}_k \Delta u(k) + \dots + \tilde{B}_{k+N_c-1} \Delta u(k+N_c-1) \\ &\vdots \\ \tilde{\chi}(k+N_P|k) &= \alpha(k, N_P-1, 0) \tilde{\chi}(k) + \alpha(k, N_P-1, 1) \tilde{B}_k \Delta u(k) + \dots + \alpha(k, N_P-1, N_c) \tilde{B}_{k+N_c-1} \Delta u(k+N_c-1) \end{aligned}$$

where

$$\alpha(k, N, j) = \prod_{i=j}^N \tilde{A}_{k+i} \quad (22)$$

in addition,  $N_c < N_P$ . In order to predict the state and output of the system at the future  $N_P$  steps, we assume that the current time is  $k$ ,  $k > 0$ , and the state variable vector  $\tilde{\chi}(k)$  represent the current system information which can be measured through observer. We assume that the control input is held constant beyond  $N_c$  steps, i.e.,  $\Delta u(k+j) = 0$ ,  $j = N_c, N_c+1, \dots, N_P-1$ . Thus, the prediction input vector  $\Delta U_a(k)$  can be defined:

$$\Delta U_a(k) \stackrel{\text{def}}{=} \begin{bmatrix} \Delta u(k) \\ \Delta u(k+1) \\ \vdots \\ \Delta u(k+N_c-1) \end{bmatrix}_{N_c \times 1} \quad (21)$$

Combining (15) with (21) presents predictive state variable at each future step, it is shown in Eq. (22) at the bottom of this page. Using the current state information,

we define the output  $\tilde{Y}_a(k)$  at  $N_P$  steps presented in Eq. (23).

$$\tilde{Y}_a(k) \stackrel{\text{def}}{=} \begin{bmatrix} \tilde{Y}(k+1) \\ \vdots \\ \tilde{Y}(k+N_c) \\ \vdots \\ \tilde{Y}(k+N_P) \end{bmatrix}_{N_P \times 1} \quad (23)$$

The outputs over the prediction horizon  $N_P$  can be derived by combining (18), (19), (21), (22), and (23), shown as in Eq. (24).

$$\tilde{Y}_a(k) = \psi \tilde{\chi}_a(k) + \Theta \Delta U_a(k) \quad (24)$$

where

$$\tilde{\chi}_a(k) = \tilde{\chi}(k) \quad (25)$$

$$\psi = [\tilde{C}_k \tilde{A}_k \tilde{C}_k \tilde{A}_{k+1} \tilde{A}_k \dots \tilde{C}_k \alpha(k, N_P-1, 0)]^T \quad (26)$$

### C. CONSTRUCTION OF COST FUNCTION

The purpose of MPC-based tracking strategy is to ensure the error between the predicted output variables and the reference values as small as possible, which means vehicles can follow the predetermined trajectory accurately and obtain lateral

stability. Therefore, the cost function can be constructed as follows [22], [23]:

$$J_k = \| Q \left[ \tilde{Y}_a(k) - \tilde{Y}_{a,\text{ref}}(k) \right] \|^2 + \| R \Delta U_a(k) \|^2 \quad (28)$$

where  $Q$  and  $R$  are weighting matrices of the controlled outputs and inputs, which are presented in Eq. (29) and Eq. (30) respectively.

$$Q = \begin{bmatrix} Q_1 & 0 & \cdots & 0 & \cdots & 0 \\ 0 & Q_2 & \cdots & 0 & \cdots & 0 \\ \vdots & \vdots & \ddots & \vdots & \vdots & \vdots \\ 0 & 0 & \cdots & Q_{N_c} & \cdots & 0 \\ \vdots & \vdots & \vdots & \vdots & \ddots & \vdots \\ 0 & 0 & \cdots & 0 & \cdots & Q_{N_p} \end{bmatrix}$$

$$Q_i = \begin{bmatrix} Q_\varphi & 0 \\ 0 & Q_Y \end{bmatrix}, \quad i = 1, 2, \dots, N_p \quad (29)$$

$$R = \begin{bmatrix} R_0 & 0 & \cdots & 0 \\ 0 & R_1 & \cdots & 0 \\ \vdots & \vdots & \ddots & \vdots \\ 0 & 0 & \cdots & R_{N_c-1} \end{bmatrix}$$

$$R_i = [R_{\Delta\delta}], \quad i = 1, 2, \dots, N_c - 1 \quad (30)$$

The reference matrix  $\tilde{Y}_{a,\text{ref}}(k)$  is defined as Eq. (31), which consists of the reference location and the heading angle in prediction horizon.

$$\tilde{Y}_{a,\text{ref}}(k) \stackrel{\text{def}}{=} \begin{bmatrix} \tilde{Y}_{\text{ref}}(k+1) \\ \tilde{Y}_{\text{ref}}(k+2) \\ \vdots \\ \tilde{Y}_{\text{ref}}(k+N_p) \end{bmatrix} \quad (31)$$

The constraints dealt with the controlled variables and imposed on the output are considered in the MPC-based upper decision controller, shown as follows:

$$\Delta U_{\min} \leq \Delta U_a(k) \leq \Delta U_{\max} \quad (32)$$

$$U_{\min} \leq U_a(k) \leq U_{\max} \quad (33)$$

$$\tilde{Y}_{\min} \leq \tilde{Y}_a(k) \leq \tilde{Y}_{\max} \quad (34)$$

where  $\Delta U_{\min}/\Delta U_{\max}$  represents minimum / maximum values of the angular increment of front wheel,  $U_{\min}/U_{\max}$  shows minimum / maximum of front wheel angle,  $\tilde{Y}_{\min}$  and  $\tilde{Y}_{\max}$  are minimum and maximum of output respectively. Combining Eq. (20) with Eq. (33), we obtain:

$$U_{\min} \leq A \Delta U_a(k) + U(k-1) \leq U_{\max} \quad (35)$$

$$\Theta = \begin{bmatrix} \tilde{C}_k \tilde{B}_k & 0 & \cdots & 0 \\ \tilde{C}_k \tilde{A}_k \tilde{B}_k & \tilde{C}_k \tilde{B}_k & \cdots & 0 \\ \vdots & \vdots & \ddots & \vdots \\ \tilde{C}_k \alpha(k, N_c - 1, 1) \tilde{B}_k & \tilde{C}_k \alpha(k, N_c - 1, 2) \tilde{B}_{k+1} & \cdots & \tilde{C}_k \tilde{B}_{k+N_c-1} \\ \vdots & \vdots & \ddots & \vdots \\ \tilde{C}_k \alpha(k, N_p - 1, 1) \tilde{B}_k & \tilde{C}_k \alpha(k, N_p - 1, 2) \tilde{B}_{k+1} & \cdots & \tilde{C}_k \alpha(k, N_p - 1, N_c) \tilde{B}_{k+N_c-1} \end{bmatrix} \quad (27)$$

where

$$U(k-1) = \begin{bmatrix} u(k-1) \\ u(k-1) \\ \vdots \\ u(k-1) \end{bmatrix}_{N_c \times 1} \quad (36)$$

$$A = \begin{bmatrix} 1 & 0 & 0 & \cdots & 0 \\ 1 & 1 & 0 & \cdots & 0 \\ 1 & 1 & 1 & \cdots & 0 \\ \vdots & \vdots & \vdots & \ddots & \vdots \\ 1 & 1 & 1 & \cdots & 1 \end{bmatrix}_{N_c \times N_c} \quad (37)$$

#### D. SOLUTION BASED ON QUADRATIC PROGRAMMING

Quadratic programming is an optimization problem with quadratic objective function and constraints, which is widely applied in optimizing the cost function of MPC-based controller. The cost function (28) can be reconstructed in a standard quadratic form, shown as follows:

$$J_k = \frac{1}{2} \Delta U_a(k)^T H \Delta U_a(k) + G \Delta U_a(k) \quad (38)$$

where

$$H = 2\Theta^T Q \Theta + R, \quad G = 2\tilde{E}_a^T(k) Q \Theta$$

$$\tilde{E}_a(k) = \psi \tilde{Y}_a(k) - \tilde{Y}_{a,\text{ref}}(k) \quad (39)$$

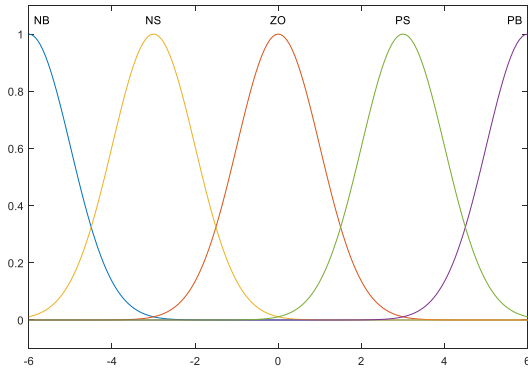
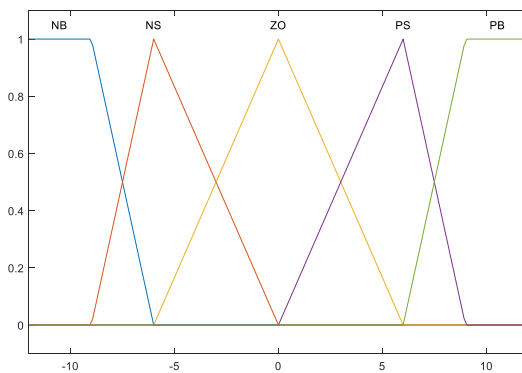
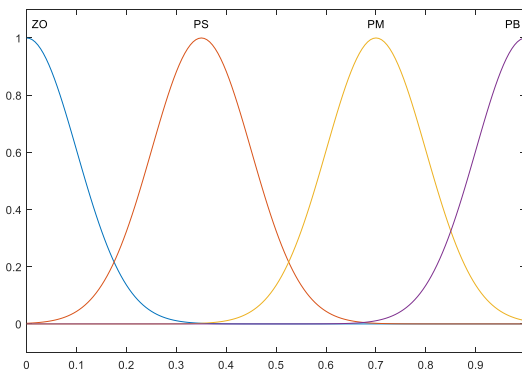
A series of optimal control inputs are calculated in the control horizon by solving the following optimization problem:

$$\begin{aligned} & \min_{\Delta U_a(k)} J_k \\ & \text{subj. to } \Delta U_{\min} \leq \Delta U_a(k) \leq \Delta U_{\max} \\ & \quad U_{\min} \leq A \Delta U_a(k) + U(k-1) \leq U_{\max} \\ & \quad \tilde{Y}_{\min} \leq \tilde{Y}_a(k) \leq \tilde{Y}_{\max} \end{aligned} \quad (40)$$

We define optimal control input vector by  $\Delta U_a^*(k) = [\Delta u^*(k), \Delta u^*(k+1), \dots, \Delta u^*(k+N_c-1)]$ , the front wheel steering angle calculated by upper MPC-based decision controller is  $u(k) = u(k-1) + \Delta u^*(k)$ , which will be acting on vehicle actuators until the generation of optimal control inputs at the next moment.

#### IV. WEIGHT ADAPTIVE CONTROL

In the process of path tracking experiment based on classical MPC controller, a problem about ride comfort appears, which refers to that the steering wheel of the vehicle is revised dramatically in a short time because of the pursuit of tracking accuracy when the vehicle is far from the target trajectory. An

(a) The membership function of the input  $e_Y$ (b) The membership function of the input  $e_\varphi$ 

(c) The membership function of the outputs

**FIGURE 2.** The membership functions of input and output variables.

improved MPC controller based on fuzzy adaptive control is proposed to guarantee both tracking accuracy and ride comfort, which can adjust the weights of cost function adaptively based on lateral position error and heading error.

Fuzzy logic control (FLC) can mimic human driver's procedural knowledge to achieve intelligent control behavior and response, which can be divided into three phases: fuzzification, fuzzy inference, and defuzzification [24]. In the first step, the current input values are fuzzified into linguistic or fuzzy values with a certain degree of authenticity depending on relevant membership functions. Then, those fuzzy values could be converted into the fuzzy output values through some

**TABLE 2.** Fuzzy rules of weight on Lateral error.

		$e_Y$				
		NB	NS	ZO	PS	PB
$e_\varphi$	NB	ZO	PS	PM	PS	ZO
	NS	ZO	PS	PM	PS	ZO
	ZO	PS	PM	PB	PM	PS
	PS	ZO	PS	PM	PS	ZO
	PB	ZO	PS	PM	PS	ZO

**TABLE 3.** Fuzzy rules of weight on Heading error.

		$e_\varphi$				
		NB	NS	ZO	PS	PB
$e_Y$	NB	PB	PM	PS	PS	ZO
	NS	PM	PS	ZO	PS	ZO
	ZO	PS	ZO	ZO	PM	PS
	PS	PM	PS	ZO	PS	ZO
	PB	PB	PM	PS	PS	ZO

**TABLE 4.** Fuzzy rules of weight on angular increment of front wheel.

		$r_{R_{\Delta\delta}}$				
		NB	NS	ZO	PS	PB
$e_Y$	NB	PM	PS	ZO	PS	PM
	NS	PB	PM	PS	PM	PB
	ZO	PB	PM	PS	PM	PB
	PS	PB	PM	PS	PM	PB
	PB	PM	PS	ZO	PS	PM

certain fuzzy rules. The outputs will be de-fuzzified into actual outputs finally [25].

According to the fuzzy variable base, two fuzzy control inputs including lateral position error  $e_Y$  and heading error  $e_\varphi$  are defined, which represent the error between current lateral position and the reference position and the error between current heading angle and the reference. Considered the allowable vehicle moving states in path tracking, all inputs of fuzzy controller can be fuzzified into five fuzzy sets: NB (negative big), NS (negative small), ZO (zero), PS (positive small), PB (positive big). Three weight ratios about  $Q_\varphi$ ,  $Q_Y$ , and  $R_{\Delta\delta}$  in Eq. (28) are presented as the outputs of fuzzy controller, shown in Eq. (41). Similarly, considering the weight is always non-negative, the output is fuzzified into four fuzzy sets: PB (positive big), PM (positive medium), PS (positive small), ZO (zero).

$$\begin{aligned} r_{Q_\varphi} &= Q_\varphi / Q_{\varphi,max}, \quad r_{Q_\varphi} \in [0, 1] \\ r_{Q_Y} &= Q_Y / Q_{Y,max}, \quad r_{Q_Y} \in [0, 1] \\ r_{R_{\Delta\delta}} &= R_{\Delta\delta} / R_{\Delta\delta,max}, \quad r_{R_{\Delta\delta}} \in [0, 1] \end{aligned} \quad (41)$$

The membership functions associated with the inputs and outputs of fuzzy controller are shown as in Fig. 2.

Fuzzy rule base contains fuzzy rules considering correlations between the inputs and the outputs, which are constructed by people's driving experience taking into

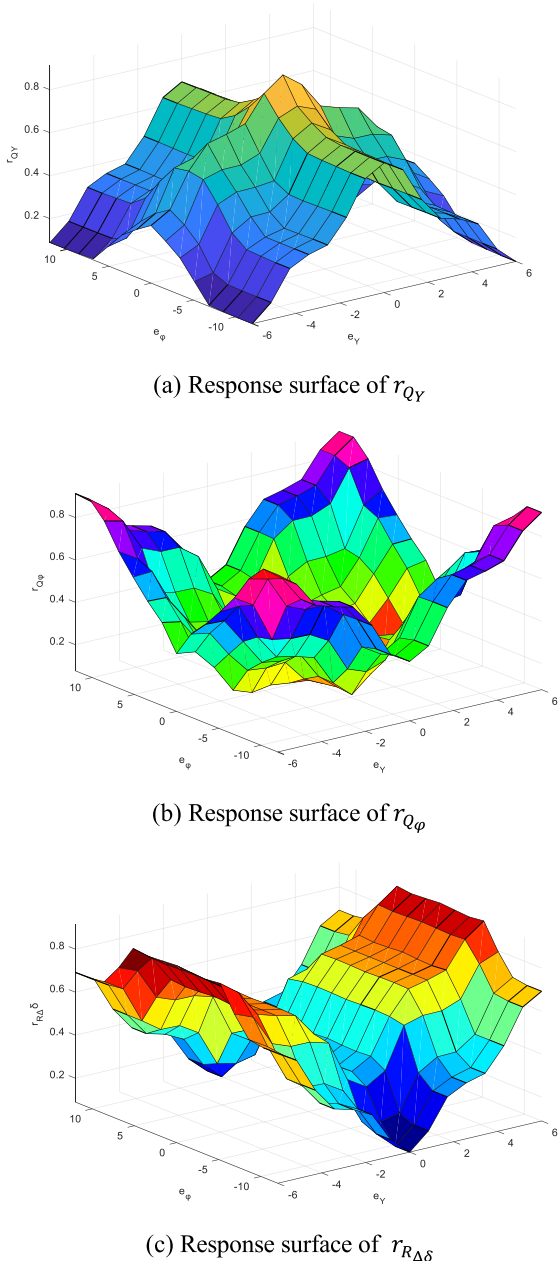


**FIGURE 3.** Response surfaces of fuzzy controllers. (a), (b), and (c) represent the outputs of  $r_{QY}$ ,  $r_{Q\phi}$ , and  $r_{R\Delta\delta}$  through fuzzy rules respectively.

consideration both tracking accuracy and ride comfort when tracking the predetermined path, as listed in Tables 2–4.

Fig. 3 shows the response surfaces which present the relationship between the outputs and the inputs under fuzzy rules. Through the above-mentioned fuzzy rules, when far from the target path, the weight on increment of wheel angle control will be increased to ensure ride comfort as the vehicle approaches the predetermined path.

## V. SIMULATION AND ANALYSIS

To verify the effectiveness of the proposed improved MPC controller, the CarSim-Matlab/Simulink co-simulations are

conducted and analysed as shown in Fig. 4. Two different scenarios are constructed in this section: one scenario refers to that the initial position of the autonomous vehicle coincides with the starting point of the predetermined trajectory, in which the performance comparison between the designed controller and pure-pursuit controller is presented. And the other is when the vehicle is far from the target trajectory, the driving comfort problem caused by the classical MPC controller is solved by the proposed improved MPC controller. TABLE 5 shows parameters of the vehicle model.

### A. SCENARIO 1

Fig. 5–9 show the comparison between the proposed improved MPC controller and the pure-pursuit controller [26] in tracking performance, lateral error, front wheel angle and lateral dynamic stability. We observe that both methods can control the vehicle to track the desired path accurately as shown in Fig. 5. In Fig. 6, the proposed improved MPC controller displays a better path-tracking accuracy than that of the pure-pursuit controller, though the maximum lateral error is  $0.243\text{ m}$  for proposed controller and  $0.211\text{ m}$  for the other. Ensuring the driving stability of vehicles is the major advantage of the proposed improved MPC controller, which can be concluded from Fig. 7. MPC-based controller can change the front steering angle smoothly when the vehicle is tracking the desired trajectory, which guarantees the continuity and smoothness of driving. On the contrary, the front steering angle will change violently in a short time when the pure-pursuit controller works ( $0\text{ s} < t < 9\text{ s}$ ). As a result, the driving comfort is low. Meanwhile, from Fig. 8 and 9, the sideslip angle and yaw rate of the vehicle fluctuate seriously under the pure-pursuit controller, which indicates that the vehicle is in unstable lateral stability state. On the contrary, the improved MPC controller can guarantee the lateral stability in path tracking process.

Considering the aforementioned simulation results, we conclude that both controllers can make the vehicle track the predetermined trajectory accurately. However, it should be noted that a better path-tracking performance with smooth front steering angle is obtained by using the proposed improved MPC controller.

### B. SCENARIO 2

In Scenario 2, the initial position of the vehicle is away from the planned path, which is in line with the practical situation because of the disturbance of the GPS signal. We set the initial position of the vehicle as the point A( $-2, -4$ ) in the inertial coordinate system. The driving process can be divided into two parts: the first one (from point A to point B in Fig. 10) is the path-approaching, and the second one (after point B) is the process of accurate tracking. The weight coefficients of classical MPC controller are set as follows:  $Q_\phi = 1$ ,  $Q_Y = 10$ ,  $R_{\Delta\delta} = 1$ . The proposed improved MPC controller can adaptively adjust the weights of different constraints in the cost function to balance the contradiction between tracking accuracy and ride comfort.

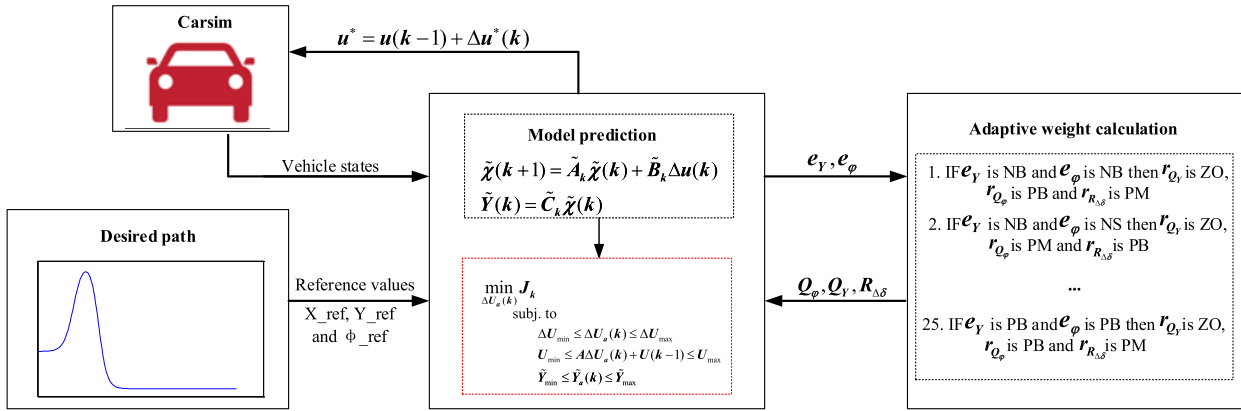


FIGURE 4. Overall architecture for path tracking.

TABLE 5. Vehicle model parameters.

$m$ (kg)	$I_z$ (kg · m <sup>2</sup> )	$l_f$ (m)	$l_r$ (m)	$v$ (m/s)
1350	4000	1.016	1.562	10

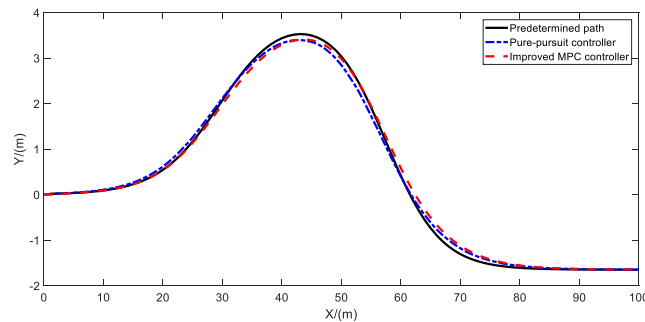


FIGURE 5. Predetermined path and tracking path in scenario 1.

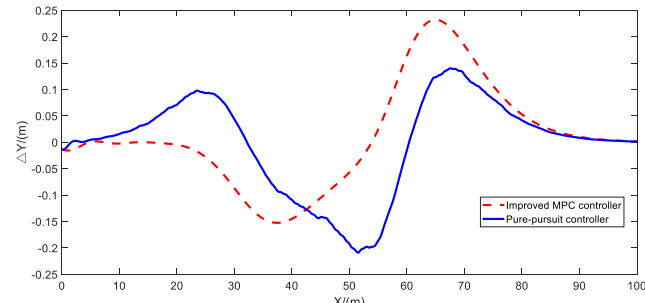


FIGURE 6. Lateral tracking error in scenario 1.

The classical MPC controller blindly pursues the tracking accuracy in the process of path tracking, which results in the high frequency angle change of front wheel in a short time when the vehicle is far from the target path, as shown in the black box in Fig. 12. The weights of the cost function are dynamically adjusted by the improved controller through the fuzzy adaptive algorithm. That is to say, when the lateral

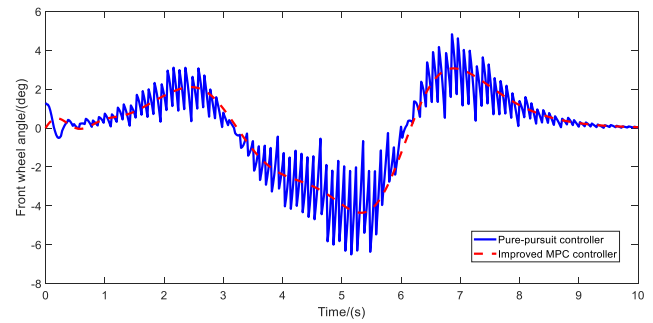


FIGURE 7. Front steering angles in scenario 1.

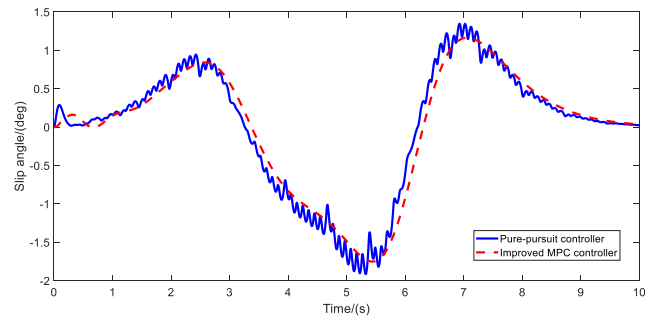


FIGURE 8. Slip angles in scenario 1.

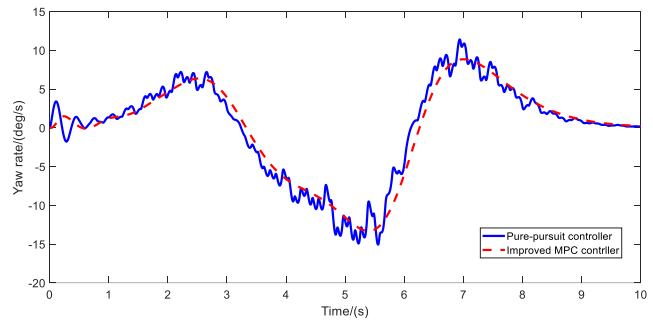


FIGURE 9. Yaw rate in scenario 1.

error is too large, the weight of the ride comfort constraint is increased to ensure that the vehicle is smoothly approaching the predetermined path. Of course, that will result in partial

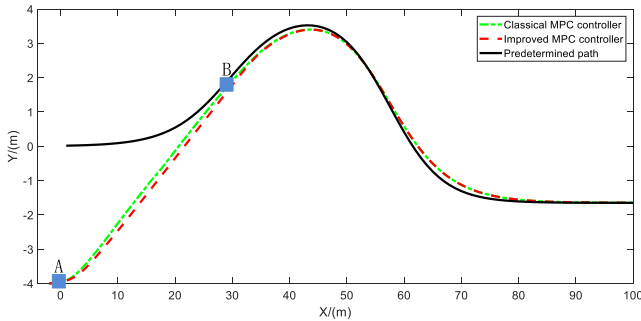


FIGURE 10. Predetermined path and tracking path in scenario 2.

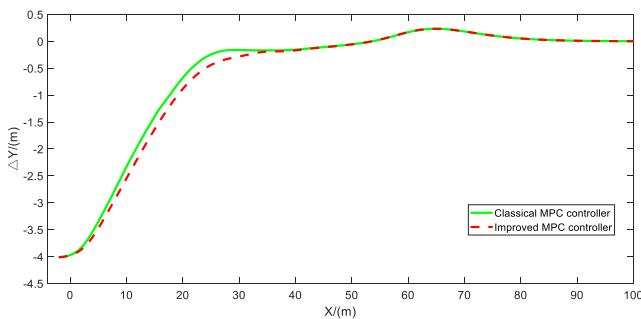


FIGURE 11. Lateral tracking error in scenario 2.

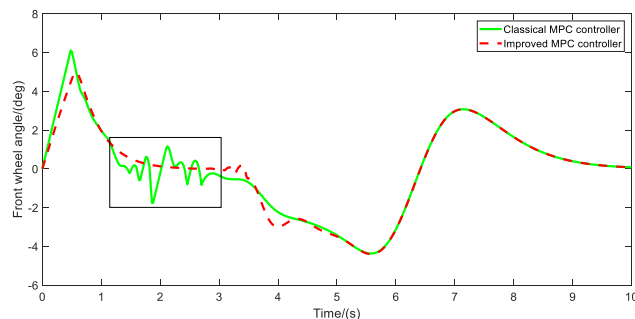


FIGURE 12. Front steering angles in scenario 2.

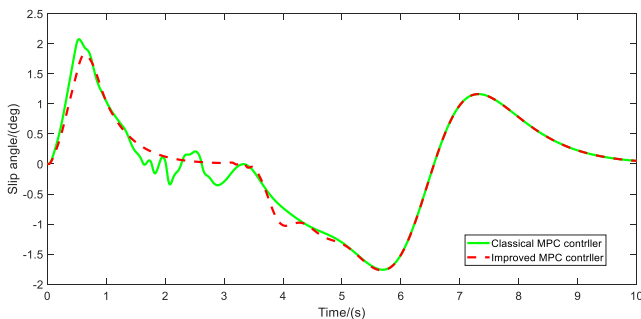


FIGURE 13. Slip angles in scenario 2.

loss of tracking accuracy (the maximum difference of lateral error is about 0.18 m) as shown in Fig. 11. Fig. 13 and 14 show the sideslip angle and yaw angular velocity of the vehicle controlled by the classical MPC controller fluctuate greatly in the process of path-approaching. The improved

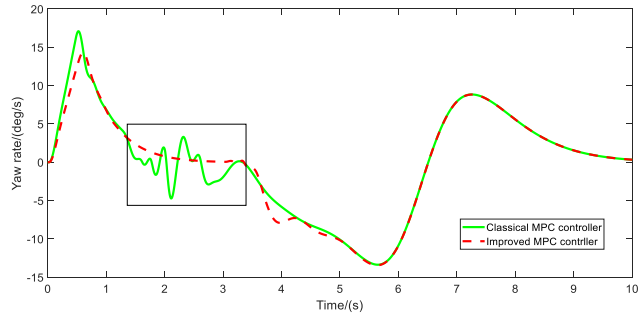


FIGURE 14. Yaw rate in scenario 2.

TABLE 6. Performance analysis of the three controllers.

	Pure-pursuit controller	Classical MPC controller	Improved MPC controller
Tracking accuracy	High	High	High
Ride comfort	Bad	Bad in the path-approaching	Good
Lateral stability	Bad	Bad in the path-approaching	Good

MPC controller guarantees the lateral stability in the whole process of path tracking.

Under the condition of guaranteeing certain tracking accuracy, the improved controller can cover a better driving comfort performance than that of the classical MPC controller and the pure-pursuit controller. TABLE 6 presents the performance analysis of the three controllers.

## VI. CONCLUSION

In this paper, an improved MPC controller has been presented for path tracking control of autonomous vehicles. The proposed controller has the ability to forecast future vehicle states and minimize the gap between the reference path and the trajectory anticipated by the augmented vehicle model in a prediction horizon, and then generates the optimal steering by solving an optimal problem with multiple constraints online. Meanwhile, the improved MPC controller introduces the fuzzy algorithm into the classical MPC controller to adjust the weights of cost function constraints adaptively.

The effectiveness of the proposed controller was verified by CarSim-Matlab/Simulink co-simulations. The improved MPC algorithm was implemented in MATLAB/Simulink, and the actual plant used in the simulations was a CarSim vehicle model. Through the simulation results, the following conclusions are drawn:

- 1) High tracking accuracy can be achieved.
- 2) The improved MPC controller ensures steering smoothness and ride comfort.
- 3) The lateral dynamic stability of the vehicle is guaranteed during the whole path tracking process.

Research on vehicle autonomous driving strategy combining path planning and path tracking modules is a topic in the future.

## REFERENCES

- [1] D. González, J. Pérez, V. Milanés, and F. Nashashibi, "A review of motion planning techniques for automated vehicles," *IEEE Trans. Intell. Transp. Syst.*, vol. 17, no. 4, pp. 1135–1145, Apr. 2016.
- [2] M. G. Plessen, "Trajectory planning of automated vehicles in tube-like road segments," in *Proc. 20th Int. Conf. Intell. Transp. Syst.*, Oct. 2017, pp. 1–6.
- [3] L. Li, D. Wen, N.-N. Zheng, and L.-C. Shen, "Cognitive cars: A new frontier for ADAS research," *IEEE Trans. Intell. Transp. Syst.*, vol. 13, no. 1, pp. 395–407, Mar. 2012.
- [4] B. Paden, M. Čáp, S. Z. Yong, D. Yershov, and E. Frazzoli, "A survey of motion planning and control techniques for self-driving urban vehicles," *IEEE Trans. Intell. Veh.*, vol. 1, no. 1, pp. 33–55, Mar. 2016.
- [5] S. Kato, E. Takeuchi, Y. Ishiguro, Y. Ninomiya, K. Takeda, and T. Hamada, "An open approach to autonomous vehicles," *IEEE Micro*, vol. 35, no. 6, pp. 60–68, Nov./Dec. 2015.
- [6] G. V. Raffo, G. K. Gomes, J. E. Normey-Rico, C. R. Kelber, and L. B. Becker, "A predictive controller for autonomous vehicle path tracking," *IEEE Trans. Intell. Transp. Syst.*, vol. 10, no. 1, pp. 92–102, Mar. 2009.
- [7] E. Kayacan, H. Ramon, and W. Saeys, "Robust trajectory tracking error model-based predictive control for unmanned ground vehicles," *IEEE/ASME Trans. Mechatronics*, vol. 21, no. 2, pp. 806–814, Apr. 2016.
- [8] G. Heredia and A. Ollero, "Stability of autonomous vehicle path tracking with pure delays in the control loop," *Adv. Robot.*, vol. 21, nos. 1–2, pp. 23–50, 2007.
- [9] A. P. Aguiar and J. P. Hespanha, "Trajectory-tracking and path-following of underactuated autonomous vehicles with parametric modeling uncertainty," *IEEE Trans. Autom. Control*, vol. 52, no. 8, pp. 1362–1379, Aug. 2007.
- [10] S. Chaib, M. S. Netto, and S. Mammar, " $H_\infty$  adaptive, PID and fuzzy control: A comparison of controllers for vehicle lane keeping," in *Proc. IEEE Intell. Vehicles Symp.*, Jun. 2004, pp. 139–144.
- [11] J. E. Normey-Rico, I. Alcalá, J. Gómez-Ortega, and E. F. Camacho, "Mobile robot path tracking using a robust PID controller," *Control Eng. Pract.*, vol. 9, no. 11, pp. 1209–1214, 2001.
- [12] J. E. Naranjo, C. Gonzalez, R. Garcia, and T. D. Pedro, "Lane-change fuzzy control in autonomous vehicles for the overtaking maneuver," *IEEE Trans. Intell. Transp. Syst.*, vol. 9, no. 3, pp. 438–450, Sep. 2008.
- [13] W. Yihu, S. Dandan, H. Zhixiang, and Y. Xiang, "A fuzzy control method to improve vehicle yaw stability based on integrated yaw moment control and active front steering," in *Proc. Int. Conf. Mechatronics Automat.*, Aug. 2007, pp. 1508–1512.
- [14] S. Cheng, L. Li, M.-M. Mei, Y.-L. Nie, and L. Zhao, "Multiple-objective adaptive cruise control system integrated with DYC," *IEEE Trans. Veh. Technol.*, vol. 68, no. 5, pp. 4550–4559, May 2019.
- [15] J. Ji, A. Khajepour, W. W. Melek, and Y. Huang, "Path planning and tracking for vehicle collision avoidance based on model predictive control with multiconstraints," *IEEE Trans. Veh. Technol.*, vol. 66, no. 2, pp. 952–964, Feb. 2017.
- [16] S. Cheng, L. Li, H. Guo, Z.-G. Chen, and P. Song, "Longitudinal collision avoidance and lateral stability adaptive control system based on MPC of autonomous vehicles," *IEEE Trans. Intell. Transp. Syst.*, to be published.
- [17] L. Yang, M. Yue, J. Wang, and W. Hou, "RMPC-based directional stability control for electric vehicles subject to tire blowout on curved expressway," *J. Dyn. Syst., Meas., Control*, vol. 141, no. 4, 2019, Art. no. 041009.
- [18] S. Xu and H. Peng, "Design, analysis, and experiments of preview path tracking control for autonomous vehicles," *IEEE Trans. Intell. Transp. Syst.*, to be published.
- [19] C. E. Beal and J. C. Gerdes, "Model predictive control for vehicle stabilization at the limits of handling," *IEEE Trans. Control Syst. Technol.*, vol. 21, no. 4, pp. 1258–1269, Jul. 2012.
- [20] J. A. Cabrera, J. J. Castillo, J. Pérez, J. M. Velasco, A. J. Guerra, and P. Hernández, "A procedure for determining tire-road friction characteristics using a modification of the magic formula based on experimental results," *Sensors*, vol. 18, p. 896, Mar. 2018.
- [21] M. Batra, J. McPhee, and N. L. Azad, "Anti-jerk model predictive cruise control for connected electric vehicles with changing road conditions," in *Proc. 11th Asian Control Conf. (ASCC)*, Dec. 2017, pp. 49–54.
- [22] P. Falcone, F. Borrelli, J. Asgari, H. E. Tseng, and D. Hrovat, "Predictive active steering control for autonomous vehicle systems," *IEEE Trans. Control Syst. Technol.*, vol. 15, no. 3, pp. 566–580, May 2007.
- [23] F. Borrelli, P. Falcone, T. Keviczky, J. Asgari, and D. Hrovat, "MPC-based approach to activesteering for autonomous vehicle systems," *Int. J. Veh. Auton. Syst.*, vol. 3, pp. 265–291, Jan. 2005.
- [24] S. Wen, Z. Q. M. Chen, X. Yu, Z. Zeng, and T. Huang, "Fuzzy control for uncertain vehicle active suspension systems via dynamic sliding-mode approach," *IEEE Trans. Syst., Man, Cybern., Syst.*, vol. 47, no. 1, pp. 24–32, Jan. 2017.
- [25] H. Li, X. Jing, H.-K. Lam, and P. Shi, "Fuzzy sampled-data control for uncertain vehicle suspension systems," *IEEE Trans. Cybern.*, vol. 44, no. 7, pp. 1111–1126, Jul. 2014.
- [26] G. C. Rains, A. G. Faircloth, C. Thai, and R. L. Raper, "Evaluation of a simple pure pursuit path-following algorithm for an autonomous, articulated-steer vehicle," *Appl. Eng. Agricult.*, vol. 30, no. 3, pp. 367–374, 2014.



**HENGYANG WANG** received the B.E. degree in electrical engineering and automation from Beijing Jiaotong University, Beijing, China, in 2018, where he is currently pursuing the Ph.D. degree in electrical engineering with the School of Electrical Engineering. His research interests include intelligent vehicle perception and intelligent vehicle control.



**BIAO LIU** received the Ph.D. degree in electrical engineering from Beijing Jiaotong University, Beijing, China, in 2008, where he is currently an Associate Professor with the School of Electrical Engineering. His research interests include electrical control automation, network control and network communication, and intelligent vehicle control.



**XIANYAO PING** received the B.S. degree in vehicle engineering from the School of Automotive Engineering, Wuhan University of Technology, Wuhan, China, in 2018. He is currently pursuing the M.S. degree in mechanical engineering with the School of Vehicle and Mobility, Tsinghua University, Beijing, China. His research interest includes vehicle dynamics and control.



**QUAN AN** received the B.S. degree in vehicle engineering from the Harbin Institute of Technology at Weihai, Weihai, China, in 2018. He is currently pursuing the M.S. degree in vehicle engineering with the School of Vehicle and Mobility, Tsinghua University, Beijing, China. His research interests include intelligent vehicle dynamic control and hybrid electric vehicle.